9th Asia-Pacific Conference on Wind Engineering
Auckland, New Zealand
3-7 December 2017

Interference mechanism of two tall buildings in staggered arrangement

G.B. Zu[1] and K.M. Lam[2]

[1]Department of Civil Engineering, The University of Hong Kong, Pokfulam Road, Hong Kong

[2]Department of Civil and Environmental Engineering, The Hong Kong University of Science and Technology, Clear Water Bay, Hong Kong

Abstract

The instantaneous flow field around two tall buildings in a critical relative location are measured with time-resolved PIV in the wind tunnel. Wind pressures on the downstream building are measured simultaneously with PIV to explore the excitation mechanisms for the strong interference phenomenon of increased across-wind forces. The time-averaged flow patterns around the two buildings show that the wake of the downstream building exhibits an asymmetry under the effect of the upstream building. Vortex shedding patterns around the two buildings are studied by phase averaging and clear in-phase synchronization of vortices shed from the two buildings is observed.

Introduction

Numerous wind tunnel experiments have studied the interference effects between overall wind loads and wind-induced responses on two or more neighbouring buildings [1-6]. In recent years, some attention is focused on local wind pressure modification for its importance in cladding design [7, 8]. All those studies provide not just large amounts of useful data to enrich the database but also empirical formulas for evaluating local and overall wind loads for buildings under interference at certain building geometries and arrangement patterns. However, as there are many involving parameters, such as geometry and arrangement of buildings, terrain type and turbulence intensity of approaching flow, possible combinations of these parameters are too large to be covered exhaustively. Therefore, a more physically-based approach, such as investigating the underlying mechanisms of interference effect, would be worth adopting to solve the problem. Some efforts have been made to understand various interference mechanisms from flow field visualization [9, 10]. Despites these studies, the exact interference mechanisms between two high-rise buildings still remain not clear.

In the present study, the flow field around two staggered tall buildings in a critical arrangement is measured by time-resolved particle image velocimetry (TR-PIV) while synchronized pressure measurement is made on the downstream building. The result is compared with the flow field around an isolated building. The phase averaging technique is employed to determine the phase of the coherent structures around the two buildings aiming to bring about a better understanding of the interference effect.

Experimental Setup

Experiments were carried out in the boundary layer wind tunnel in the Department of Civil Engineering at the University of Hong Kong. Tests were carried out under a simulated wind flow of the open land terrain at a geometric scale of 1:1000, where the mean wind speed profile followed the power law with a power exponent of 0.11. The mean wind speed and turbulence intensity at the roof height of the building model were 5.5 m/s and 0.089, respectively. Two building models of identical sizes and shapes were used in the experiments. Measurements were made on a rigid pressure model, referred to as the principal building, while the other model was not installed with any instrument, referred to as the interfering building. Both building models had a square-plan form of breadth D = 30 mm. The height-to-breadth ratio was H/D = 6. At the target geometric scale 1:1000, the models represented full-scale buildings of height 180 m and width 30 m. The Reynolds number of the testing was $Re = U_H D/\upsilon \approx 1.14\times10^4$. A total of 120 pressure taps, 30 on each of its four surfaces, were installed on the walls of the principal building (Fig. 1). The PIV system used to measure the velocity fields has been described in our previous study [11]. In order to synchronize the surface wind pressure measurement and the flow field acquisition by PIV, pressure measurements with a scanning system were triggered by the framing signals of the PIV camera. This synchronization ensured that the pressure scanning was made at the same instant with the PIV realizations. The sampling frequency of both PIV images and wind pressures was 100 Hz.

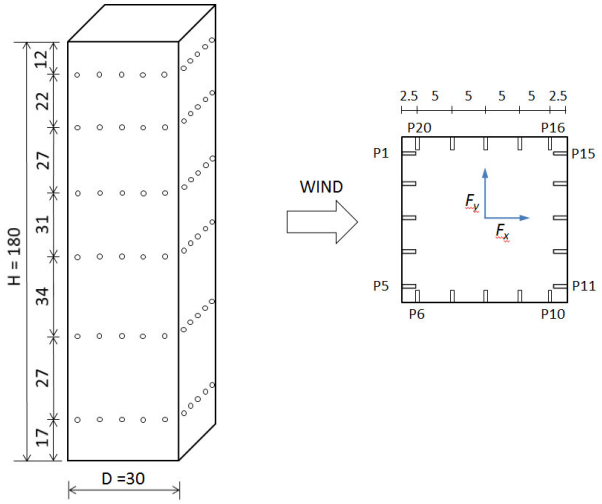

Figure 1. Layout of pressure taps on principal building model (unit: mm)

Result and discussion

From the measured pressure signals on the four walls of the principal building, aerodynamic forces acting on the model were calculated by means of pressure integration. This paper focus on the across-wind moment which was obtained as follows:

$$M_c(t) = \sum_{i=1}^{N} p_i(t) A_i n_{i,cross} h_i \qquad (1)$$

where p_i, A_i and h_i are the pressure, tributary area and height, respectively of pressure tap i, and $n_{i,cross}$ is the component of the unit normal of A_i along the across-wind loading direction.

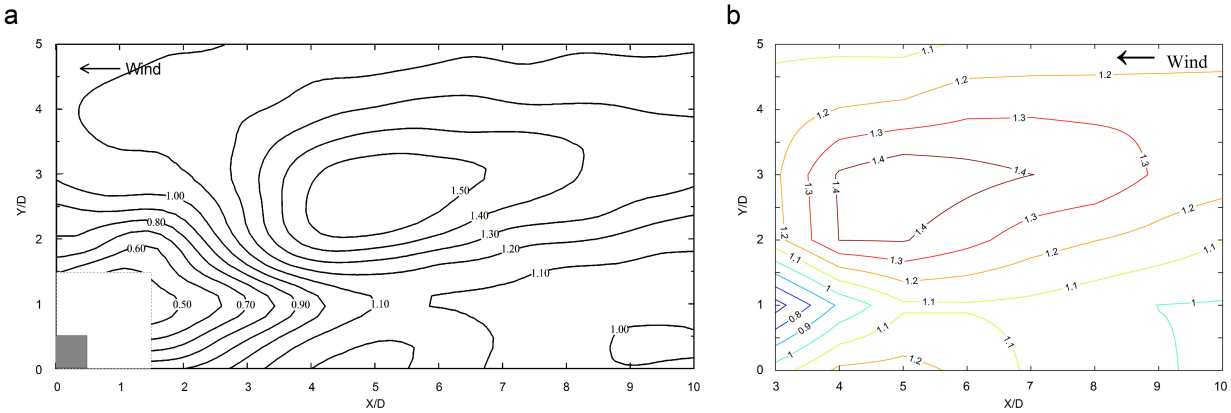

Figure 2. IF contours of RMS across-wind moment: (a) present study; (b) Mara, Terry [12].

The interference effects on the aerodynamic wind load on the principal building are summarized in the form of interference factor (IF) that depicts the change of aerodynamic force acting on the principal building due to interference from surrounding buildings [13]. In the present experiments, contours of IF for the RMS (root-mean-square) across-wind moment are presented in Fig. 2(a). The result of a previous study [12] is shown in Fig. 2(b) for comparison. Generally, two studies agree well with each other despites the difference in geometric scales of tests. A well-defined region is observed in the staggered arrangement where IF is higher than unity. The peak location is found at (X/D = 5, Y/D = 2.5) where the greatest IF equals 1.61. This location of peak IF reported in Mara et al. [12] is (X/D = 5, Y/D = 3) and the peak IF is between 1.4 and 1.5. It should be noted that in that study the interval of spacing variations is D instead of $D/2$ used in the present study. It is known that a higher approaching turbulence tends to lower the level of interference. It is thus believed that the larger IF observed in the present study is mainly an effect of the lower free-stream turbulence intensity than in Ref. [14].

The excitation mechanism behind the strong interference on across-wind moment of the principal building under the critical staggered location (X/D = 5, Y/D = 2.5) is explored from the results of synchronized PIV and pressure measurements.

As a start, the time-averaged mean streamlines of wind load around the building in the isolated singe building configuration are presented in Fig. 3a. This is on a horizontal plane at height Z/H = 0.5. As expected, a predominantly symmetric flow pattern is obtained. The wind flow is observed to separate at the leading edges of the side walls and a pair of oval counter-rotating vortices is observed in the building wake. The extent of the recirculating wake is indicated by the saddle point to reach a location at approximately x/D = 2.2.

When the interfering building is located at the critical upwind location (Fig. 3b), a distinctively different wake pattern is observed on downstream principal building. The mean flow approaching the building is shifted in a slightly sideway direction (or upward direction in the figure). As a result, the counter-clockwise vortex at the lower side wall is suppressed largely by the upwards-shifted shear layer, while, the clockwise vortex, which is supposed to appear near the upper side, is impaired dramatically in the time averaged sense. The recirculating region of the wake now occupies a smaller space up to a length of 1.7D from the centre of the building. As for the upstream building, the building wake pattern remains largely unchanged, compared with the isolated building case.

However, the fluctuating across-wind force on the downstream building, which is believed to be mainly induced by vortex excitation, is largely magnified at this location. The moment spectra, shown in Fig. 4, show that the spectral distribution of the across-wind force of the principal building is even more concentrated around the Strouhal peak than the isolated building case, indicating a more pronounced periodicity. There seems to be a contradiction between the observed mean flow field and the across-wind force fluctuations.

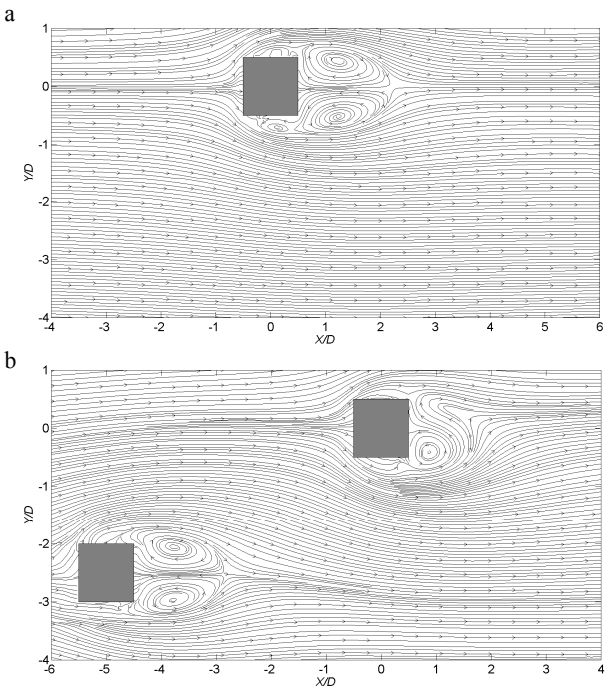

Figure 3. Time-averaged streamlines: (a) isolated single building; (b) two buildings at X/D = 5, Y/D = 2.5.

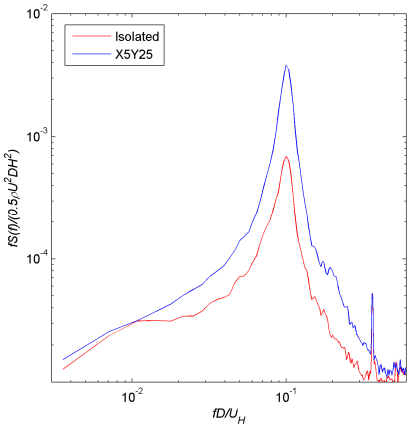

Figure 4. Across-wind spectra of principal buildiing in isolated single building situation and under interference from upwind building

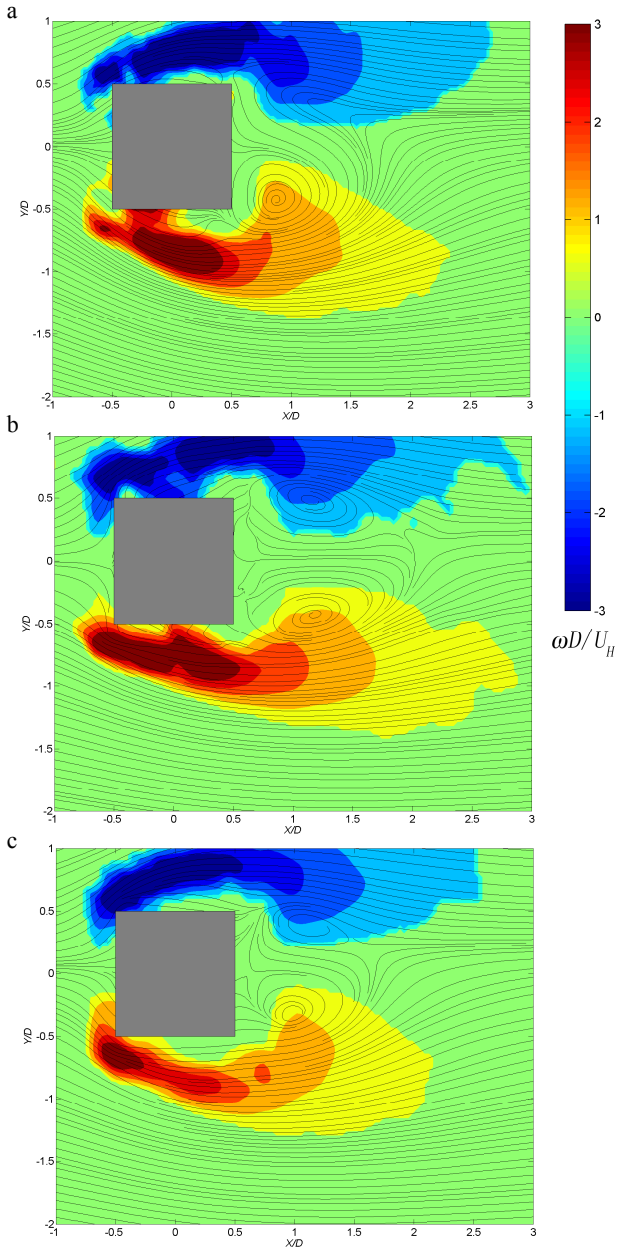

Figure 5. Time-averaged flow fields of the near wake, streamlines and vorticity contours: (a) X/D = 5, Y/D = 2.5; (b) X/D = 5, Y/D = 4.5; (c) X/D = 9, Y/D = 2.5

Figure 5 presents the time-averaged streamlines in the near wake of the downstream building with the upstream building at three different upstream locations: (X/D = 5, Y/D = 2.5) ,(X/D = 5, Y/D = 4.5) and (X/D = 9, Y/D = 2.5). For the focused critical configuration, the wake region dwindles, with a length about x/D = 2.2 from the centre of the building, and the saddle point is found to be located near the upper side surface instead of the centreline. With a larger lateral distance 4.5D, the near wake pattern returns approximately to the undisturbed state of an isolated single building (Fig. 3a). The effect of streamwise building separation is also checked. For a relatively large separation X = 9D, it is found that although the flow pattern becomes more symmetric than the critical configuration, the influence of the upstream building wake is still present for the fact that the length of the building wake is shorter and the saddle point is found to be higher than the centreline.

In order to reveal the dominant fluctuating flow phenomenon responsible for the excitation of across-wind moment at the focused critical configuration (X/D = 5, Y/D = 2.5), the phase-averaged technique [14] is applied to the time-resolved PIV velocity data. Several candidates can be chosen as the reference signal from which the phase of the flow can be determined and the across-wind force on the principal building acting on the height of PIV measurement plane is used in the present study.

The across-wind moment spectrum shown in Fig. 4 exhibits a peak at a dimensionless frequency (Strouhal number) $St = nD/UH \approx 0.10$ corresponding to periodic vortex shedding at the frequency of 18 Hz (model scale). From the fluctuating across-wind force measured with pressure integration on the principal building, the phase of the flow is determined using the Hilbert transform technique [14]. The Hilbert transform allows the calculation of the instantaneous envelope and phase from a band limited signal $r(t)$ such as the across-wind force signal in this study:

$$\hat{r}(t) = \frac{1}{\pi}\int_{-\infty}^{\infty}\frac{r(\xi)}{\xi - t}d\xi \qquad (2)$$

where complex function is obtained $z(t) = r(t) - i\hat{r}(t)$ which can be written in the form of $A(t)e^{\varphi(t)}$ where $A(t)$ is the instantaneous envelope of $r(t)$, and $\varphi(t)$ is the instantaneous phase. To improve the signal analysis, a band pass filter with a band pass 10–26 Hz is applied to the across-wind force signal before applying the Hilbert transform. A threshold of 30% on the period and a threshold of 0.3 on the amplitude of normalized across-wind force are applied to screen out irregular periods. After this sort, about 88% of the signal was chosen for the calculation of the phase-averaged flow fields.

The phase-averaged flow patterns at the focused critical location are shown in Fig. 6, at π/2 phase intervals. An interesting in-phase synchronization phenomenon is observed for two building wakes. At φ = 0, a counter-clockwise rotating vortex is about to be shed from the lower side of the principal downstream building. At the same time, a similar large vortex is observed at the rear side of the upstream building at almost the same phase of shedding. At φ =π/2, both vortices are shed, apparently in a synchronized manner, from the two buildings. This results in the typical "Z" shaped streamline patterns into their near wakes. On the left side of the "Z", the alternate vortex starts to grow from the opposite corner of each building. However, on the principal building, the development of this clockwise rotating vortex is not as well-established as the preceding counter-clockwise vortex. This is probably caused by the faster approaching flow on the lower side of the building due to the presence of the upstream building on the lower side.

The two clockwise vortices grow and dominates the near wake regions at $\varphi = \pi$. It is worth noting that the developed vortex on the upper side of the principal building is farther from the building as compared with the alternating vortex developed from the lower side (at φ = 0). This may contribute to the asymmetric mean flow pattern of the downstream building as observed in Fig. 5a. As vortices are shed, a grossly reverse flow pattern is observed at $\varphi = 3/2\pi$, compared with that at $\varphi = \pi/2$. It is noted that the vortex patterns behind both buildings exhibit a highly synchronized relation at these two phases as well.

Conclusions

The instantaneous flow field around two buildings under interference in a critical relative location and their wind forces

are measured simultaneously with synchronized PIV and pressure measurements in the wind tunnel. The time-averaged flow pattern is compared with that of isolated building and different configurations. It is found that the presence of the upstream building leads to disturbed and asymmetric wake pattern of the downstream building in time averaging sense. The phase-resolved vortex shedding processes from the two buildings are obtained by the phase-averaging technique on the quasi-periodic across-wind force fluctuations on the principal downstream building. An in-phase synchronization of the vortex shedding from both buildings is observed and this is believed to be the cause of largely amplified across-wind excitation of the principal building.

Acknowledgments

The study is supported by a research grant awarded by the Research Grants Council of Hong Kong (HKU 713813E).

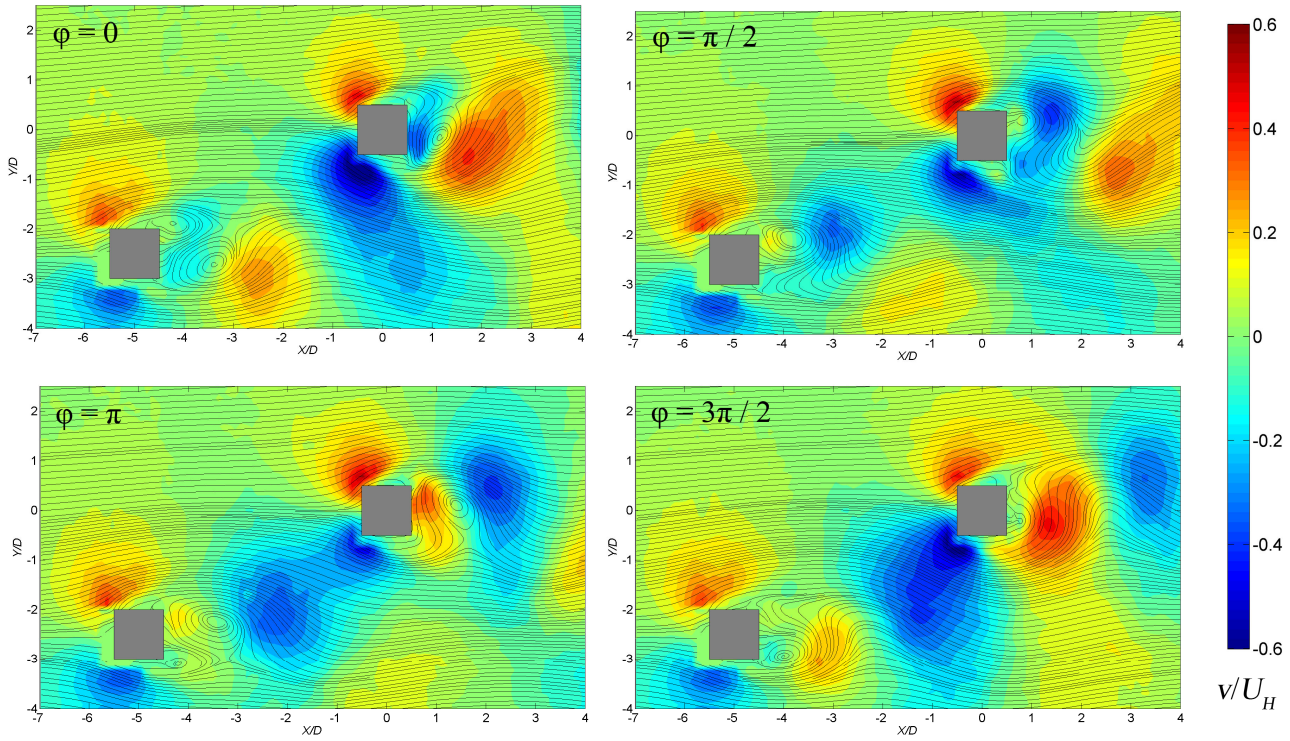

Figure 6. Phase-resolved flow fields

Reference

[1] Bailey, P.A. and K.C.S. Kwok, *Interference excitation of twin tall buildings.* J. Wind Eng. Ind. Aerodyn., 1985. **21**(3): p. 323-338.

[2] Taniike, Y., *Interference mechanism for enhanced wind forces on neighboring tall buildings.* J. Wind Eng. Ind. Aerodyn., 1992. **42**(1-3): p. 1073-1083.

[3] Xie, Z.N. and M. Gu, *Simplified formulas for evaluation of wind-induced interference effects among three tall buildings.* J. Wind Eng. Ind. Aerodyn., 2007. **95**(1): p. 31-52.

[4] Lam, K.M., M.Y.H. Leung, and J.G. Zhao, *Interference effects on wind loading of a row of closely spaced tall buildings.* J. Wind Eng. Ind. Aerodyn., 2008. **96**(5): p. 562-583.

[5] Khanduri, A.C., T. Stathopoulos, and C. Bedard, *Wind-induced interference effects on buildings - a review of the state-of-the-art.* Engineering Structures, 1998. **20**(7): p. 617-630.

[6] English, E.C. and Fricke, F.R., *The interference index and its prediction using a neural network analysis of wind-tunnel data.* J. Wind Eng. Ind. Aerodyn., 1999. **83**(1-3): p. 567-575.

[7] Kim, W., Y. Tamura, and A. Yoshida, *Interference effects on local peak pressures between two buildings.* J. Wind Eng. Ind. Aerodyn., 2011. **99**(5): p. 584-600.

[8] Yu, X.F., Xie, Z.N., Zhu, J.B. and Gu, M., *Interference effects on wind pressure distribution between two high-rise buildings.* J. Wind Eng. Ind. Aerodyn., 2015. **142**: p. 188-197.

[9] Hui, Y., Tamura, Y., Yoshida and A. Kikuchi, H., *Pressure and flow field investigation of interference effects on external pressures between high-rise buildings.* J. Wind Eng. Ind. Aerodyn., 2013. **115**: p. 150-161.

[10] Sakamoto, H. and H. Haniu, *Aerodynamic forces acting on two square prisms placed vertically in a turbulent boundary-layer.* J. Wind Eng. Ind. Aerodyn., 1988. **31**(1): p. 41-66.

[11] Cheng, L. and Lam K.M., *Simultaneous measurement of wind velocity field and wind forces on a rectangular building.* In: The 14th International Conference on Wind Engineering, Porto Alegre, Brazil., 2015.

[12] Mara, T.G., Terry, B.K., Ho, T.C.E. and Isyumov, N., *Aerodynamic and peak response interference factors for an upstream square building of identical height.* J. Wind Eng. Ind. Aerodyn., 2014. **133**(0): p. 200-210.

[13] Saunders, J.W. and W.H. Melbourne, *Buffeting effects of twin upstream buildings.* 5th International Conference on Wind Engineering, Fort Collins, 1980: p. 83-86.

[14] Wlezien, R.W. and J.L. Way, *Techniques for the Experimental Investigation of the Near Wake of a Circular Cylinder.* AIAA Journal, 1979. **17**(6): p. 563-570.